

Spectrophotometry of Very Bright Stars in the Southern Sky

Kevin Krisciunas,^{1,2} Nicholas B. Suntzeff,^{1,2} Bethany Kelarek,¹ Kyle Bonar,¹ and Joshua Stenzel¹

ABSTRACT

We obtained spectra of 26 bright stars in the southern sky, including Sirius, Canopus, Betelgeuse, Rigel, Bellatrix, and Procyon, using the 1.5-m telescope at Cerro Tololo Inter-American Observatory and its grating spectrograph RCSPEC. A 7.5 magnitude neutral density filter was used to keep from saturating the CCD. Our spectra are tied to a Kurucz model of Sirius with $T = 9850$ K, $\log g = 4.30$, and $[\text{Fe}/\text{H}] = +0.4$. Since Sirius is much less problematic than using Vega as a fundamental calibrator, the synthetic photometry of our stars constitutes a Sirius-based system that could be used as a new anchor for stellar and extragalactic photometric measurements.

Subject headings: Stars - spectra

1. Introduction

Flux calibration, whether it be for photometry or spectroscopy, is a fundamental aspect of observational astronomy (Hearnshaw 1996, 2014). Vega (α Lyr) has been a fundamental photometric and spectroscopic standard for decades (Hayes & Latham 1975; Bohlin 2014; Bohlin, Gordon, & Tremblay 2014). In the 1980's the *Infrared Astronomy Satellite* (IRAS) discovered circumstellar material around Vega. Subsequently, observations with the *Spitzer Space Telescope* characterized this material as a debris disk (Su et al. 2005, 2013). Vega may be spectroscopically variable as well (Butkovskaya 2014). Bohlin (2014) comments on the *non*-variability of Vega. In any case Vega is problematic as a fundamental calibrator.

The Sloan Digital Sky Survey committed to using four principal photometric standards (Fukugita et al. 1996), but in the end relied primarily on the star BD +17°4708. Recently, it

¹Texas A. & M. University, Department of Physics & Astronomy, 4242 TAMU, College Station, TX 77843; krisciunas@physics.tamu.edu

²George P. and Cynthia Woods Mitchell Institute for Fundamental Physics & Astronomy

was revealed that this star brightened by 0.04 mag in the *UBVR* bands from 1986 to 1991 (Bohlin & Landolt 2015).

Here we present a set of bright spectrophotometric standards, many of the brightest stars visible in the southern hemisphere during the southern summer. Our data expand the lists of stars observed by Hamuy et al. (1992, 1994) and Stritzinger et al. (2005). Given the increase in sensitivity of instrumentation over the years, it might be the first time in 40 years that carefully calibrated spectra of most of these bright stars have been obtained. Using well defined bandpasses (Bessell 1990), we can use our spectra to generate *BVRI* photometry tied to a model of Sirius, which is a “well behaved” star compared to Vega.

2. The Target Stars

The target stars are situated from -70° to $+9^\circ$ declination, and all but one have right ascensions ranging from ~ 5 to 13 hours (see Fig. 1 and Table 1). About half the target stars are members of binary or multiple star systems. α CMa (Sirius) and α Car (Canopus) are the two brightest stars in the night sky. ζ Ori is the brightest O-type star in the sky.

Two other notable stars are ϵ CMa and β CMa. The former was the brightest star in the sky 4.7 million years ago (with visual magnitude -3.99). The latter was the brightest star in the sky 4.4 million years ago (with visual magnitude -3.65). This was not due to changes in their *intrinsic* luminosities. It was due to their changing *distances* from the Sun (Tompkin 1998).

α Ori (Betelgeuse) is a variable star. On the basis of 17 years of photoelectric photometry by one of us (KK), we found that its *V*-band magnitude ranges from 0.27 to 1.00 (Krisciunas 1982, 1990). A photoelectric light curve obtained from 1979 through 1996 is shown in Fig. 2. The mean brightness during these years was $V = 0.58$.

On the basis of all sky photometry and differential photometry with respect to ϕ^2 Ori, it appears that HR 1790 (γ Ori; Bellatrix) ranges in brightness in the *V*-band by as much as 0.07 mag (Krisciunas & Fisher 1988).

Only three of our targets (β Ori, α CMa, and α CMi) are fundamental *UBV* standards of Johnson & Morgan (1953). Their targets are primarily northern hemisphere objects.

3. Data Acquisition and Reduction

Three nights were allocated to this project on the CTIO 1.5-m telescope in January of 2003, and eight more nights were allocated in January of 2005. However, due to a variety of hardware and weather programs, we only obtained useful data on two nights, 6 January 2003 and 21 January 2005 (UT). On the first night all the spectra were taken with the blue grating. On the second night all the spectra were taken with the red grating.

Details of the facility spectrograph RCSPEC are discussed by Stritzinger et al. (2005). The blue and red gratings give dispersions of 2.85 and 5.43 Å per pixel, respectively. Stritzinger et al. (2005) give 5.34 Å per pixel as the dispersion of the red grating, but this is a transcription error. The FWHM values are 8.6 Å for the blue grating and 16.4 Å for the red grating. Because of the extreme brightness most of our stars, we included a 7.5 mag neutral density filter in the light path to prevent saturation of the pixels. Our exposure times ranged from 5 to 420 seconds. While the spectra of Landolt standards obtained by Stritzinger et al. (2005) are useful at wavelengths as short as 3100 Å, ours are no good below 3300 Å.

Raw two dimensional spectra were saved as FITS files 1274 by 140 pixels in size. Batches of four spectra were taken of each star, with the telescope offset 30 arcsec west along the slit between spectra to place the spectrum on a different part of the chip. A He-Ar-Ne arc spectrum was taken before every batch.³ Once the star was centered in a 2" slit, the slit width was widened to 21". Since many of our targets are close binary or multiple stars, this means that many of our spectra are blended spectra of more than one star. On the plus side, such a wide slit eliminates any worries about guiding and seeing, allowing accurate spectrophotometry under clear sky conditions.

Spectra were reduced in the IRAF environment.⁴ We made extensive use of the spectroscopic reduction manual of Massey, Valdes, & Barnes (1992). We first bias subtracted, trimmed, and flattened the spectra. One dimensional spectra were extracted with *apall* in the APEXTRACT package.⁵

³For calibration line identification we used A CCD Atlas of Helium/Neon/Argon Spectra, by E. Carder, which can be downloaded at <https://www.noao.edu/kpno/KPManuals/henear.pdf>.

⁴IRAF is distributed by the National Optical Astronomy Observatory, which is operated by the Association of Universities for Research in Astronomy, Inc., under cooperative agreement with the National Science Foundation (NSF).

⁵IRAF users should know or be reminded that there is a second version of *apall* in the CTIOSLIT part of IMRED. Setting the many parameters in one version of *apall* does not set them in the other parameter list!

Wavelength calibration was accomplished using *identify*, *reidentify*, and *dispcor* in the CTIOSLIT package. Once we had carried out the wavelength calibration we could ask the question: To what extent were our two useable nights clear? To do this one can sum up the instrumental counts over some wavelength range, then take $-2.5 \log_{10}$ of the counts to produce instrumental magnitudes. In Fig. 3 we show these instrumental magnitudes vs. airmass from 27 Sirius spectra obtained on 6 January 2003. We have eliminated the 9 spectra that were the final spectra of the batches of four on this date. For reasons we do not understand the final spectrum of each batch often gave an instrumental magnitude that was about ~ 0.10 mag fainter than the other three. In Fig. 3 the slope is 0.237 ± 0.009 mag per airmass. The RMS residual of the fit is ± 0.018 mag, which is comparable to CCD photometry on a photometric night. The wavelength range for integrating those spectra was 3600 to 5500 Å. This is somewhat wider than the standard *B*-band filter. From photometry at Cerro Tololo and Las Campanas we find a mean *B*-band extinction coefficient of 0.262 ± 0.007 mag per airmass. The bottom line is that by using RCSPEC as a photometer, we demonstrated that 6 January 2003 was clear the whole night.

Similar considerations for the spectra taken on 21 January 2005 indicate that this night became non-photometric by 05:27 UT. We will only consider spectra taken on this night prior to this time.

The flux calibration of our spectra was carried out with tasks *standard*, *sensfunc*, and *calibrate* within the CTIOSLIT package. With the *calibrate* task we applied extinction corrections appropriate for Cerro Tololo (found in file `onedstds$ctioextinct.dat` within IRAF).

For flux calibration of the blue grating spectra obtained on 6 January 2003 we observed the spectrophotometric standards HR 3454 (observed at a mean airmass of 1.201) and HR 4468 (observed at mean airmass 1.154). For red grating spectra obtained on 21 January 2005 we used the standard HR 1544 for the flux calibration. It was observed at a mean airmass of 1.427. The mean airmass values for the observations of our target stars are given in Table 1. Any systematic errors in the flux calibration with IRAF will be equal to the arithmetic *difference* of the airmass of the standards and the program stars *times* the arithmetic *difference* of the true extinction coefficient as a function of wavelength minus the adopted mean values appropriate to CTIO. For photometric sky and observations above an elevation angle of 45 degrees, any systematic error of the flux calibration should be less than 10 percent in the *B*-band and less than 5 percent in the *VRI* bands. *Relative* fluxes of our spectra and synthetic photometry have estimated internal random errors of 3 percent or better (see below).

The final step in our reduction was to tie the spectra to a Kurucz model of Sirius. An

ASCII version of an R=1000 spectrum of Sirius was kindly provided by Ralph Bohlin.⁶ The sampling is at twice the frequency of the resolution. The model spectrum has $T = 9850$ K, $\log g = 4.30$ and metallicity $[\text{Fe}/\text{H}] = +0.4$.

The wavelengths of the model spectrum were in nm, so we multiplied by 10 to convert them to Å. We also want wavelengths in air, rather than vacuum wavelengths. For this we used the transformation given at the SDSS Data Release 7 website.⁷ Finally, we used a scale factor of 2.75440×10^{-16} to convert the Kurucz model flux to that of Sirius, so that it is measured in $\text{erg cm}^{-2} \text{ s}^{-1} \text{ Å}^{-1}$.

In the top panel of Fig. 4 we see the Kurucz model spectrum. The middle panel is the average of 18 blue grating spectra of Sirius (taken at airmass less than 1.3), and 16 red grating spectra, as processed with IRAF. We have stitched together the blue grating spectra and the red grating spectra at 6000 Å, which produces a small discontinuity at that wavelength. The bottom panel of Fig. 4 is the *ratio* of the Kurucz spectrum and our mean Sirius spectrum. We call that ratio the “flux function” or “spectral flat”. All our other spectra are then multiplied by the flux function to place them on a system tied to the Kurucz model of Sirius. This largely, but not entirely, takes out the discontinuity at 6000 Å and also takes out telluric features such as the Fraunhofer B-, A-, and Z-lines at 6867, 7594 and 8227 Å, which are due to atmospheric O₂. The identity of a feature at ~ 3680 Å evident in many of our spectra is uncertain; it too is largely taken out by the spectral flat.

The average value of the flux function shown in the bottom panel of Fig. 4 is 0.990, which is close enough to 1.000 to give us confidence that the flux calibration of our coadded spectra of Sirius, obtained with IRAF, is consistent with the scaling of the model of Sirius to the flux density of the star. Our ultimate filter by filter zeropoints are the values of the *BVRI* magnitudes of Sirius given in Table 1, which come from Cousins (1971, 1980).

Fully reduced spectra, transformed to the “Sirius system” and ranging from 3300 to 10,000 Å, are shown in Fig. 5. Spectra taken with only the blue grating are shown in Fig. 6.⁸

⁶One must use a model spectrum of appropriate resolution. Otherwise the final spectra may contain spurious features such as fictitious P Cygni profiles. A scaled FITS version of the Kurucz model spectrum can be obtained via <http://www.stsci.edu/hst/observatory/crds/calspec.html> as file `sirius_mod.002.fits`. A comment in the header of this file indicates that fluxes have been scaled by 2.75440×10^{-16} . This accounts for the distance to Sirius and its limb-darkened angular diameter.

⁷ <http://classic.sdss.org/dr7/products/spectra/vacwavelength.html>

⁸ FITS and ASCII spectra are available via <http://people.physics.tamu.edu/krisciunas/spec.tar.gz> and from the online version of this paper.

Some line identifications are given in the last panel of Fig. 5. In spectra of stars hotter than the Sun we clearly see the Balmer lines at 6563, 4861, 4340, 4102 Å and shorter wavelengths. Cooler stars such as HR 3307 (ϵ Car) and HR 2061 (α Ori) show the infrared Ca^+ triplet (8498, 8542, and 8662 Å) and the blended Na D lines (5890 and 5896 Å). ζ Ori and early B-type stars, such as HR 1790 (γ Ori), HR 2294 (β CMa), HR 2618 (ϵ CMa), and HR 4853 (β Cru), show He I absorption at 4471 and 5876 Å, though it is difficult to see given the scale of the spectra shown in Figs. 5 and 6. A higher resolution spectrum of ζ Ori A from 3980 to 4940 Å, including line identifications, is shown in Fig. 14 of Soto et al. (2011).

One thing to note in our reduced spectra is the strength of the Balmer jump in early-type main sequence stars. This is due to ionization of atomic hydrogen from the first excited state, producing strong absorption shortward of the Balmer limit at 3646 Å. This results in fainter U -band magnitudes of such stars. A much weaker Balmer jump is seen in hot giant and supergiant stars. Thus, the Balmer jump gives us a photometric tool to measure a combination of the luminosity class and the local acceleration of gravity of hot stars ($\log g$). For example, an A2 V star is 0.30 mag redder in the $U - B$ color index than an A2 III star (Drilling & Landolt 2000, pp. 388-389). Kaler (1962) points out that one also needs the rotation rates of the stars to do this properly.

4. Synthetic Photometry

The filter prescriptions originally given by Bessell (1990) have been slightly modified by Bessell & Murphy (2012). We have adopted the latter. In Fig. 7 we show their filter prescriptions, multiplied by an atmospheric extinction function appropriate to Cerro Tololo, and also multiplied by a function which accounts for the principal atmospheric extinction lines. This is noticeable in the R - and I -band functions.

We then calculated synthetic $BVRI$ magnitudes of our target stars using an IRAF script written by one of us (N. B. S.). This script uses an arbitrary zero point for each filter. We adjusted the $BVRI$ zero points to given synthetic magnitudes of the scaled Sirius model spectrum that match those of Cousins (1971, 1980). If the reader chooses to adopt different $BVRI$ magnitudes of Sirius than those given in Table 1, then the synthetic magnitudes of the other stars given in the table must be adjusted up or down accordingly.

Bessell and Murphy’s V -band filter prescription extends to 7400 Å, while our blue grating spectra stop at ~ 6400 Å. We cannot obtain synthetic V -band magnitudes for the cooler stars observed only with the blue grating. However, we can obtain approximate V -

band magnitudes for the hot stars HR 2618, 3485, 4853, and 4963 by extrapolating the spectra using the Rayleigh-Jeans approximation.

Table 1 gives our synthetic *BVRI* photometry. Fig. 8 shows the differences of our synthetic photometry and the values of Cousins (1971) and Cousins (1980), as a function $B - V$ (for B and V), $V - R$ (for R), and $V - I$ (for I). There is no color term for the V -band differences, but there are non-zero colors terms for B , R , and I . At zero color there is no offset between our V -band magnitudes and those of Cousins, but in B , R , and I ours are 0.02 to 0.03 mag fainter.

From the AAVSO online light curve calculator we find that the V -band brightness of α Ori was $V = 0.398$ on 2 January 2003, and $V = 0.384$ on 7 January. The mean is $V = 0.391$, which is comparable to our synthetic V -band magnitude of 0.398 from spectra taken on 6 January 2003. This is a good sanity check. On 21 January 2005, when we took the red grating spectra, Betelgeuse’s brightness was $V = 0.436$, according to the AAVSO.

The spectra presented here and the associated synthetic photometry can function as a Sirius-based anchor for Galactic as well as extragalactic observational astronomy.

We made use of the SIMBAD database, operated at CDS, Strasbourg, France. We thank the AAVSO for the V -band photometry of Betelgeuse obtained from their database. Kenneth Luedeke and Raymond Thompson measured Betelgeuse closest to the times we took spectra. We thank Ralph Bohlin for providing an ASCII version of the Kurucz spectrum of Sirius used for the calibration, and for useful comments. We also thank James Kaler and Jesus Maíz Apellániz for comments and references.

A. Other Spectra

The spectra shown in Figs. 5 and 6 were taken under demonstrably clear sky conditions. Synthetic photometry based on these spectra is transformable to the systems of Cousins (1971) and Cousins (1980) with uncertainties of ± 0.03 mag or less. Other spectra were taken which might be of use to the reader.

In Fig. 9 we show blue grating spectra of HR 5056 (α Vir) and HR 5267 (β Cen) taken on 6 January 2003. For reasons that are not entirely clear, our synthetic photometry was too faint by ~ 0.55 mag and ~ 0.12 mag for these two stars. The most likely explanation is a misalignment of the telescope and the dome slit. We have scaled these two spectra by appropriate amounts to make them consistent with photometry of Cousins (1971).

In Fig. 10 we show red grating spectra of HR 3454 (η Hya), HR 4216 (μ Vel), and HR 4450 (ξ Hya), taken through clouds on 21 January 2005. The spectra have been scaled to make them consistent with photometry of Cousins (1980).

Finally, in Fig. 11 we show two spectra of η Carinae taken through clouds on 21 January 2005. The top spectrum is a coadd of 12 exposures of 7 seconds. Such a short exposure time was necessary to prevent saturation of the H- α line. The bottom spectrum is a coadd of 3 exposures of 240 seconds. In this spectrum H- α is saturated, but other emission lines such as the Paschen lines of hydrogen and multiple helium lines are evident with a better signal-to-noise ratio. Since η Car has such a non-stellar spectrum and we have no available R - or I -band photometry of this star at this epoch, we have not scaled our spectra like the others presented in this Appendix.

These additional spectra are available from the first author of this article.

REFERENCES

- Bessell, M. S. 1990, *PASP*, 102, 1181
- Bessell, M. S. & Murphy, S. 2012, *PASP*, 124, 140
- Bohlin, R. C. 2014, *AJ*, 147, 127
- Bohlin, R. C., Gordon, K. D., & Tremblay, P.-E. 2014, *PASP*, 126, 711
- Bohlin, R. C., & Landolt, A. U. 2015, *AJ*, 149, 122
- Butkovskaya, V. V. 2014, *Bull. Crimean Astrophys. Obs.* 110, 80
- Cousins, A. W. J. 1971, *Roy. Obs. Annals*, 7, 1
- Cousins, A. W. J. 1980, *South Afr. Astr. Obs. Circular*, 1, 234
- Drilling, J. S. & Landolt, A. U. 2000, in *Allen's Astrophysical Quantities*, 4th ed., A. N. Cox, ed., New York, Berlin, Heidelberg: Springer, pp. 381-396
- Fukugita, M., Ichikawa, T., Gunn, J. E., Doi, M., Shimasaku, K., & Schneider, D. P. 1996, *AJ*, 111, 1748
- Hamuy, M., Walker, A. R., Suntzeff, N. B., Gigoux, P., Heathcote, S. R., & Phillips, M. M. 1992, *PASP*, 104, 533
- Hamuy, M., Suntzeff, N. B., Heathcote, S. R., Walker, A. R., Gigoux, P., & Phillips, M. M. 1994, *PASP*, 106, 566
- Hayes, D. S., & Latham, D. W. 1975, *ApJ*, 197, 593
- Hearnshaw, J. B. 1996, *The Measurement of Starlight: Two Centuries of Astronomical Photometry*, Cambridge: Cambridge Univ. P.
- Hearnshaw, J. B. 2014, *The Analysis of Starlight: Two Centuries of Astronomical Spectroscopy*, 2nd ed., Cambridge: Cambridge Univ. P.
- Johnson, H. L., & Morgan, W. W. 1953, *ApJ*, 117, 313
- Kaler, J. 1962, *Zeitschrift für Astrophys.*, 56, 150
- Krisciunas, K. 1982, *IBVS* 2104
- Krisciunas, K., & Fisher, D. 1988, *IBVS* 3227

Krisciunas, K. 1990, IBVS 3477

Krisciunas, K., & Luedeke, K. D. 1996, IBVS 4355

Massey, P., Valdes, F., & Barnes, J. 1992, *A User's Guide to Reducing Slit Spectra with IRAF*

Soto, A., Maíz Apellániz, J., Walborn, N. R., Alfaro, E. J., Barbá, R. H., Morrell, N. I., Gamen, R. C., & Arias, J. I. 2011, ApJS, 193, 24

Stritzinger, M., Suntzeff, N. B., Hamuy, M., Challis, P., Demarco, R., Germany, L., & Soderberg, A. M. 2005, PASP, 117, 810

Su, K. Y. L., Rieke, G. H., Misselt, K. A., et al. 2005, ApJ, 628, 487

Su, K. Y. L., Rieke, G. H., Malhotra, R., et al. 2013, ApJ, 763, 118

Tompkin, J. 1998, Sky and Telescope, 95, no. 4, 59

Table 1. Synthetic Photometry of Target Stars

HR ^a	Name	Binary/Multiple?	Spectral Type ^b	X _{blue} ^c	X _{red} ^d	B	V	R	I
1544	π^2 Ori	N	A1Vn	1.338	1.427	4.381	4.365	4.365	4.351
1713	β Ori	N	B8 Ia:	1.085	1.144	0.200	0.224	0.173	0.148
1790	γ Ori	N	B2 III	1.253	1.352	1.425	1.635	1.756	1.888
1948/1949	ζ Ori A/B	Y	O9.7b+O9 III+B0 II-IV	1.376	1.223	1.635	1.826	1.874	1.968
2061 ^e	α Ori	N	M1-2 Ia-Iab	1.291	1.321	2.198	0.398	-0.653	-1.799
2294	β CMa	N	B1 II-III	1.316	1.123	1.761	1.996	2.126	2.265
2326	α Car	N	F0 II	1.251	1.137	-0.584	-0.726	-0.830	-0.952
2491 ^f	α CMa	Y	A1 V	1.123	1.077	-1.425	-1.420	-1.408	-1.400
2943	α CMi	Y	F5 IV-V	1.299	1.226	0.761	0.357	0.132	-0.098
3307	ϵ Car	Y	K3 III+B2: V	1.211	1.147	3.081	1.844	1.092	0.360
3685	β Car	N	A2 IV	1.428	1.305	1.674	1.661	1.693	1.690
99	α Phe	Y	K0 III	1.562	...	3.460
2618	ϵ CMa	Y	B2 II	1.226	...	1.315	1.519
2693	δ CMa	N	F8 Ia	1.172	...	2.533
3485	δ Vel	Y	A1 V	1.177	...	1.990	1.949
3634	λ Vel	N	K4.5 Ib-II	1.126	...	3.822
3748	α Hya	N	K3 II-III	1.126	...	3.415
4763	γ Cru	N	M3.5 III	1.192	...	3.160
4853	β Cru	Y	B0.5 III	1.169	...	1.050	1.241
4963	θ Vir	Y	A1 IV s+Am	1.225	...	4.392	4.364

Note. — The stars listed in the top half of the table were observed with the blue grating and the red grating. The stars in the bottom half of the table were only observed with the blue grating.

^aHarvard Revised number = catalog number in *The Bright Star Catalogue*.

^bFrom online version of *The Bright Star Catalogue*, 5th edition, 1991.

^cMean airmass for blue grating spectra obtained on 6 January 2003 UT.

^dMean airmass for red grating spectra obtained on 21 January 2005 UT.

^e α Ori is variable. See text for comments.

^f*BV* photometry from Cousins (1971). *RI* photometry from Cousins (1980).

Fig. 1.— Positions of our target stars on the sky. The numerical labels are the catalog numbers in *The Bright Star Catalogue*. Blue dots represent stars that were observed with the blue grating only. Other stars were observed with both the blue and red gratings.

Fig. 2.— V -band magnitude of α Ori from October 1979 through November 1996. Key to data points: blue dots (K. Krisciunas), green squares (D. Fisher), red triangles (K. Luedeke). Data by Fisher were published by Krisciunas & Fisher (1988). Data by Luedeke were published by Krisciunas & Luedeke (1996).

Fig. 3.— Instrumental magnitudes of Sirius vs. airmass on 6 January 2003 (UT). The Y-axis values are equal to $-2.5 \log_{10}$ of the integrated counts from 3600 to 5500 Å of spectra that have only been wavelength-calibrated.

Fig. 4.— *Top*: Kurucz model spectrum of Sirius with $R = 1000$, $T = 9850$ K, $\log g = 4.30$, and $[\text{Fe}/\text{H}] = +0.4$. *Middle*: Average of calibrated Sirius spectra taken with airmass less than 1.3. This is the output from IRAF. *Bottom*: Ratio of model spectrum of Sirius to output from IRAF. This is the “flux function” or “spectral flat” used to multiply the reduced spectra of the other stars to place the spectra on the system of the Kurucz model of Sirius. In the bottom two panels the Fraunhofer B, A, and Z lines at 6867, 7594, and 8227 Å are labeled. These are due to molecular oxygen in the Earth’s atmosphere.

Fig. 5.— Spectra of program stars observed with the blue grating and the red grating. Small spurious variations of the flux density are seen in some spectra at 6000 and ~ 7600 Å which are attributable to the method of construction of the “spectral flat”. Some line identifications are given in the last panel of this figure. See text for further information.

Fig. 6.— Spectra of program stars observed with the blue grating only.

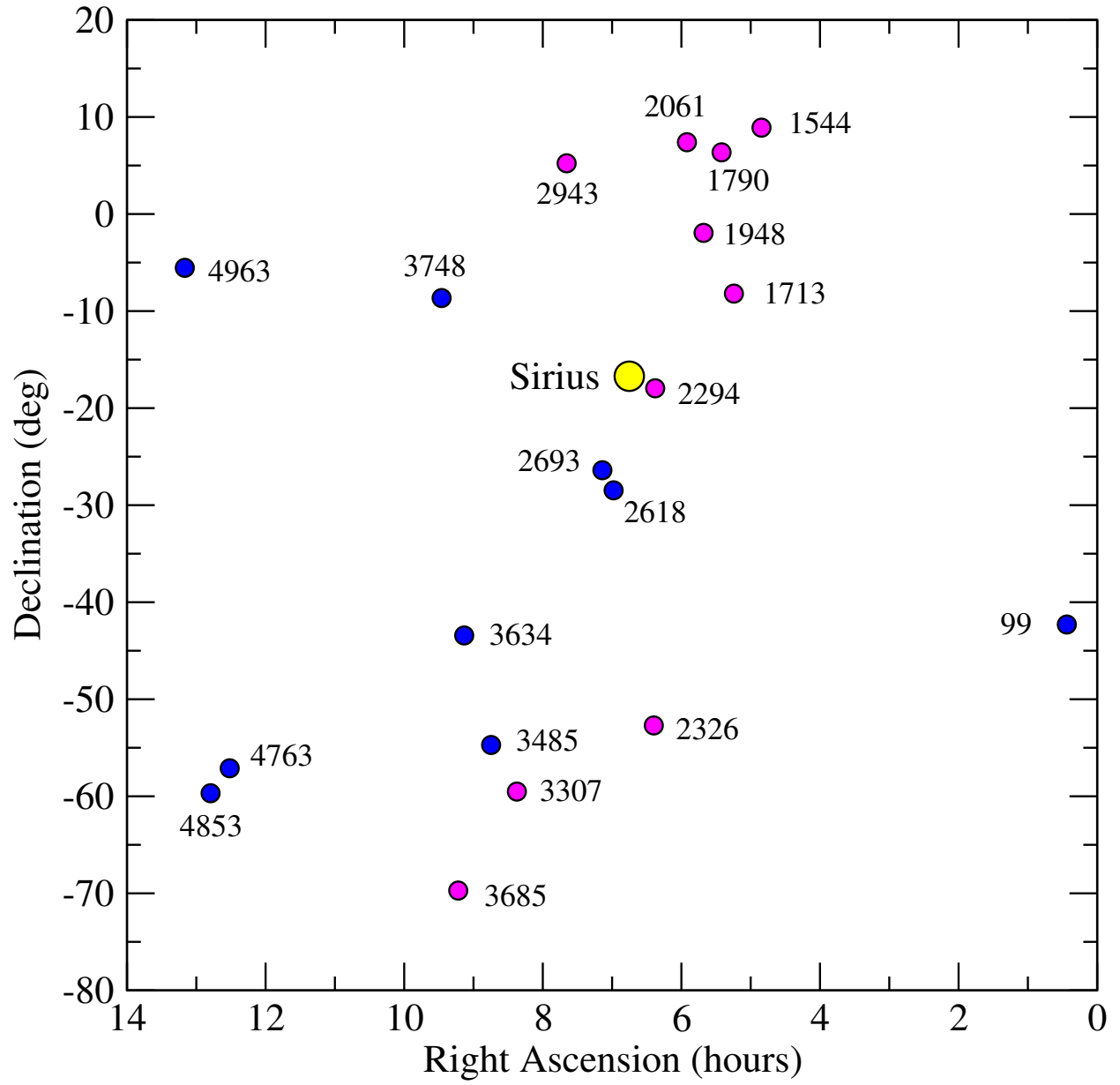
Fig. 7.— Fractional transmission of Bessell & Murphy (2012) filters, multiplied by an atmospheric extinction model appropriate to Cerro Tololo, and also multiplied by a function that accounts for principal terrestrial atmospheric features. As our spectra are not useful shortward of 3300 Å, designated here by a vertical dashed line, we can not easily obtain U -band synthetic photometry of our program stars.

Fig. 8.— Differences of photometry in the sense “our synthetic photometry” minus “photometry of Cousins”. The slope is also known as the “color term”.

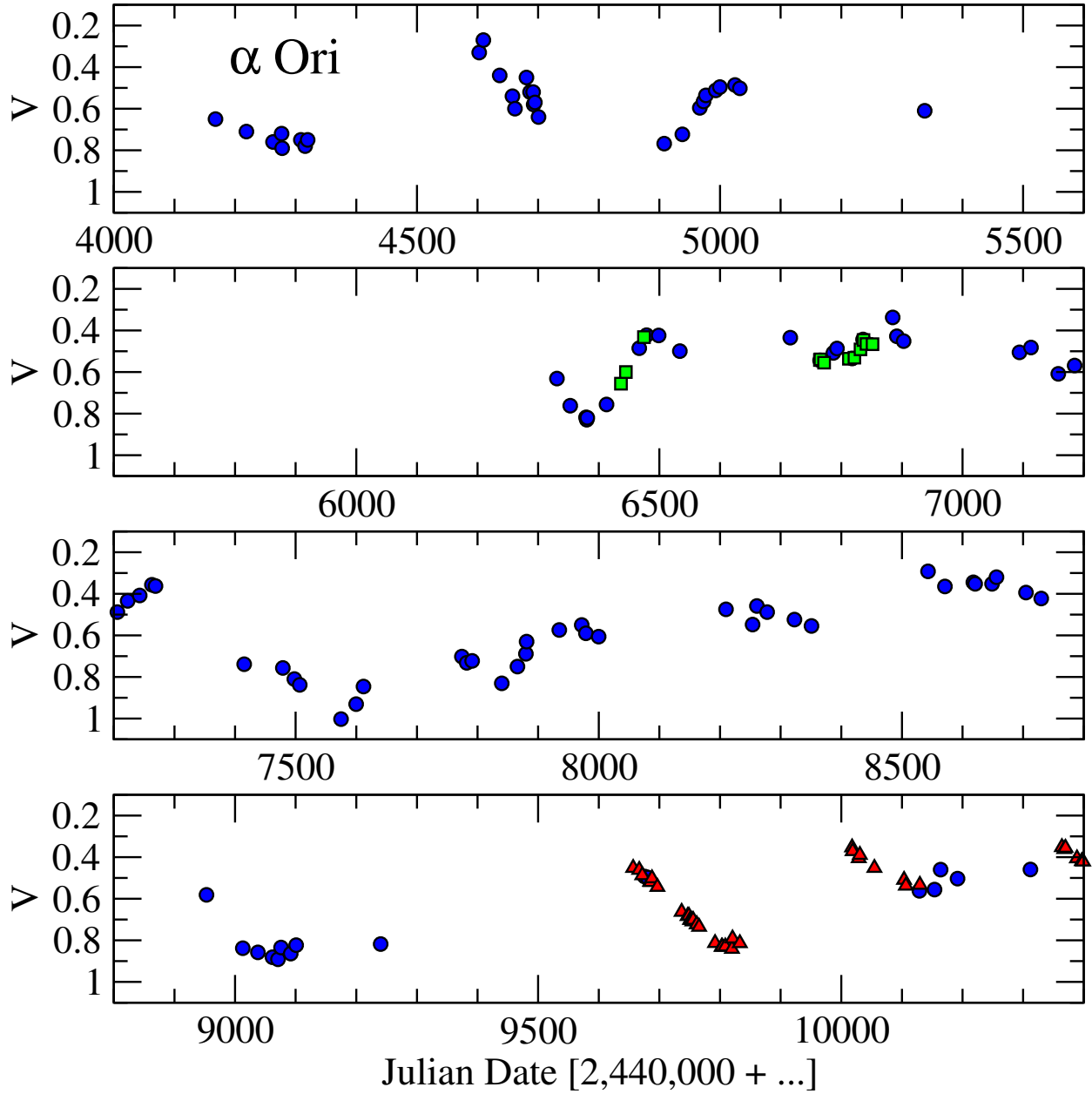
Fig. 9.— Spectra of HR 5056 (α Vir) and HR 5267 (β Cen) obtained on 6 January 2003.

Fig. 10.— Spectra of HR 3454 (η Hya), HR 4216 (μ Vel), and HR 4450 (ξ Hya) obtained on 21 January 2005 under non-photometric conditions.

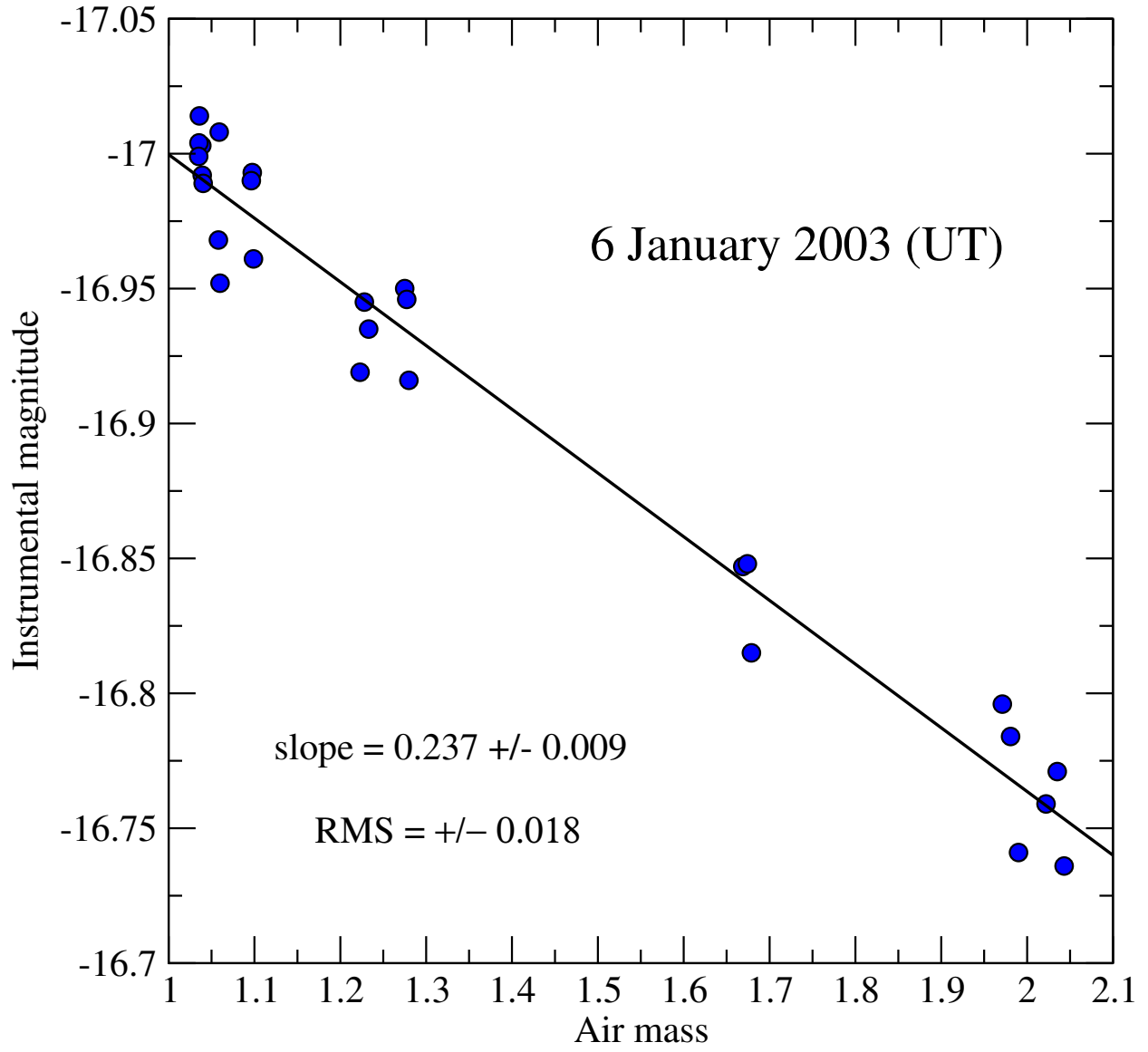
Fig. 11.— Spectra of η Carinae, obtained under non-photometric conditions on 21 January 2005. *Top*: Coadd of shorter exposures. The H- α line is not saturated. *Bottom*: Coadd of longer exposures. While the H- α line is saturated, other spectral features are more easily seen.



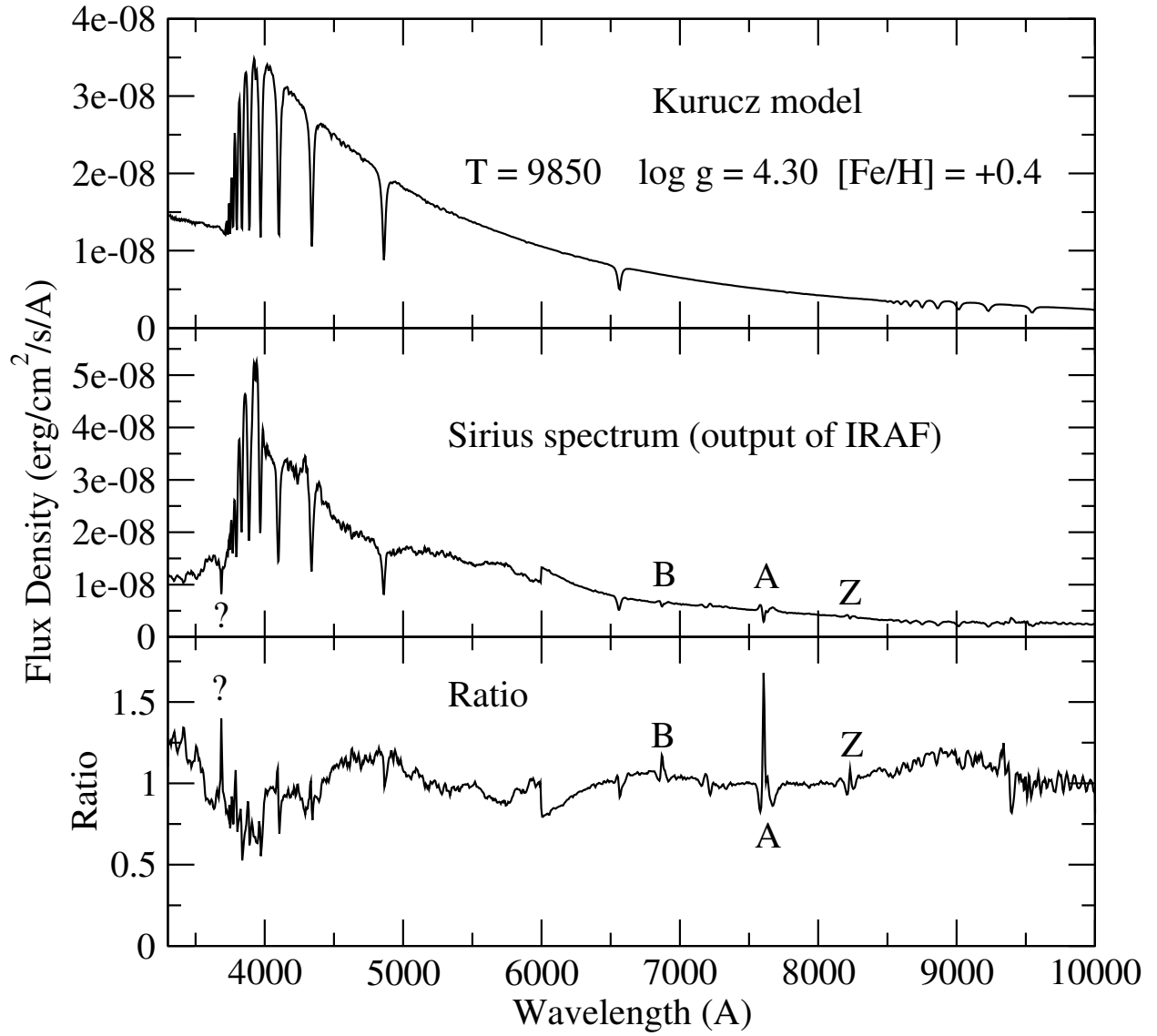
Krisciunas Fig. 1.



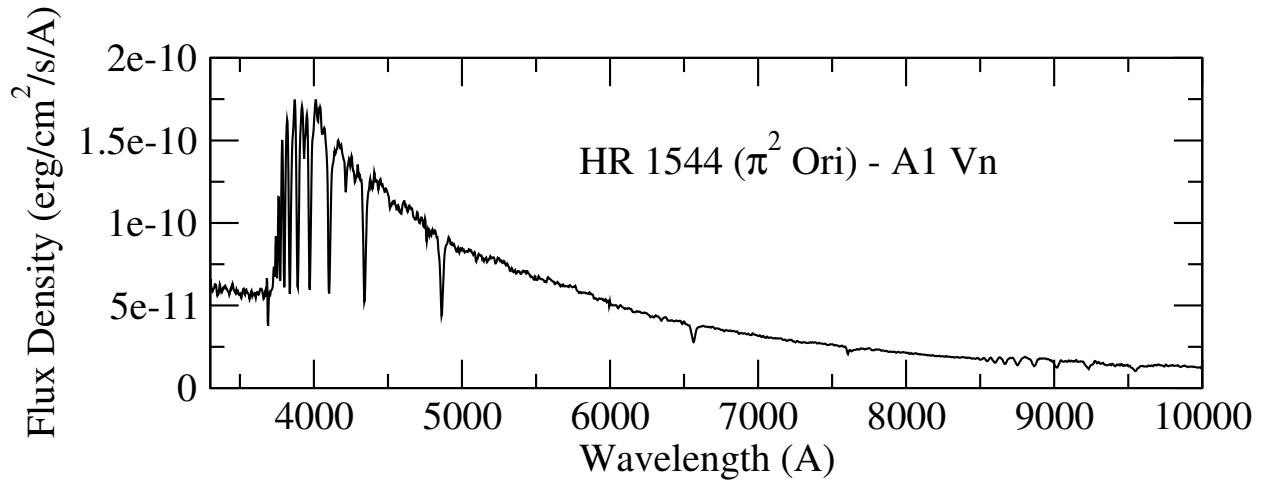
Krisciunas Fig. 2.



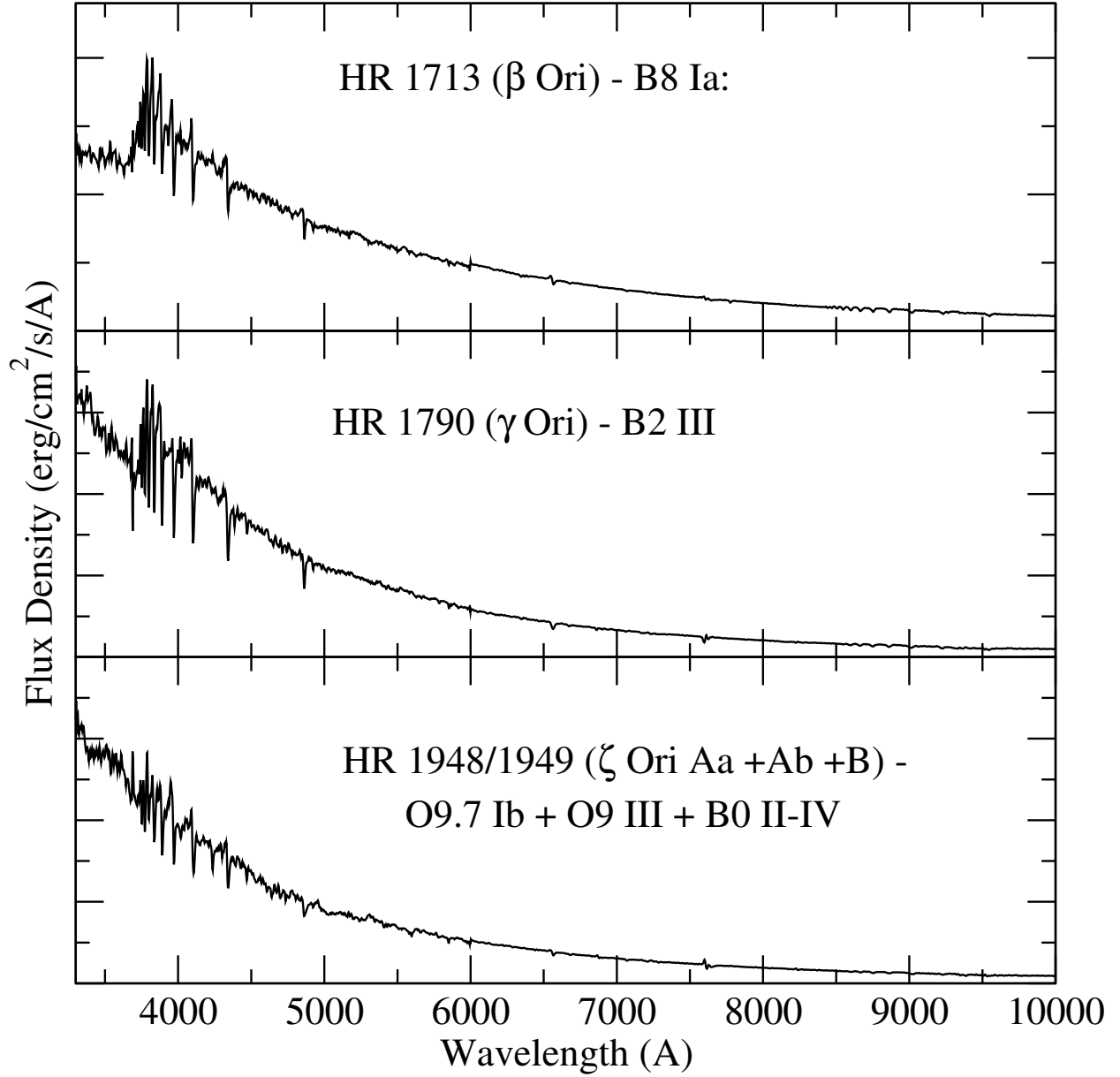
Krisciunas Fig. 3.



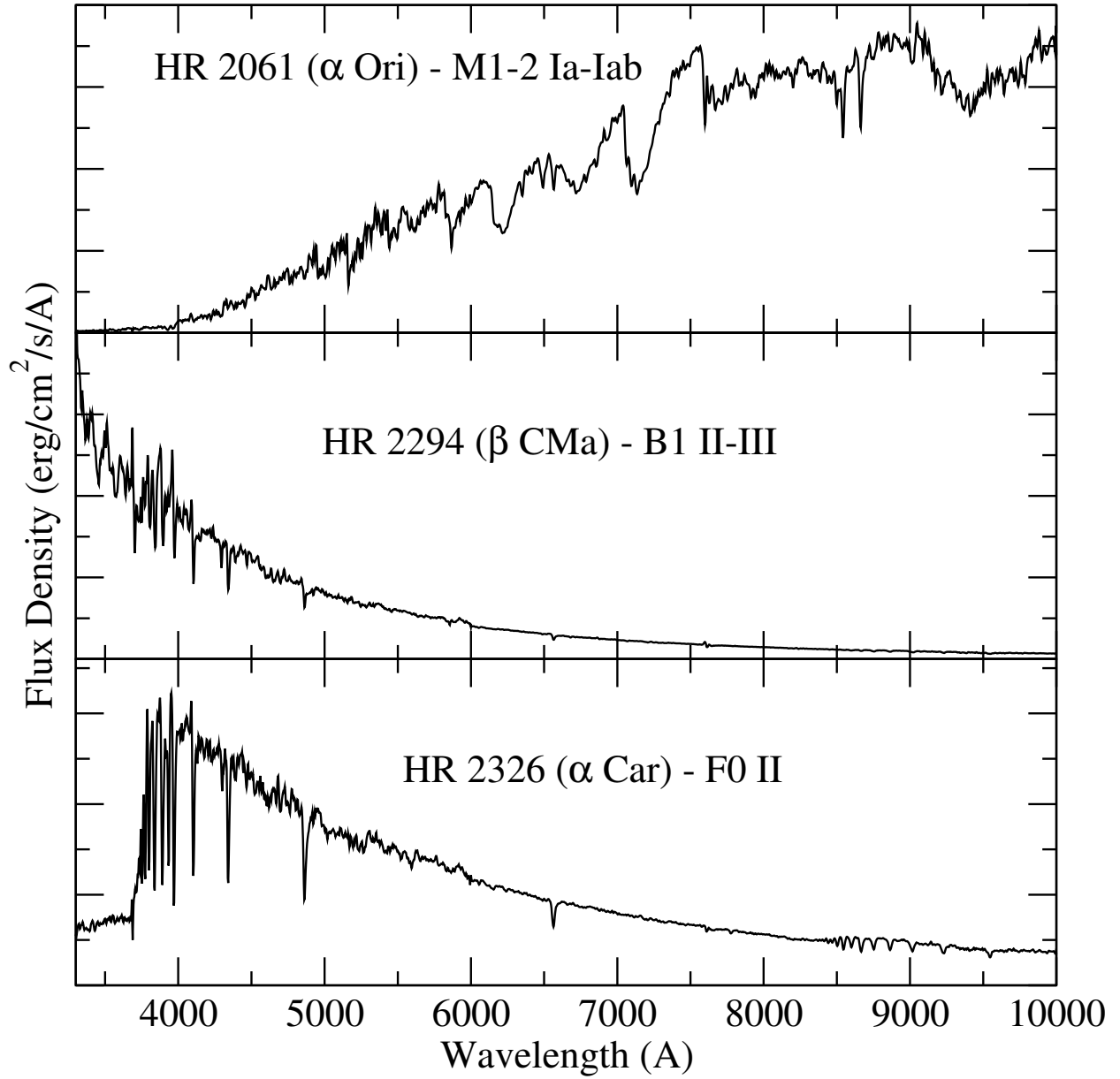
Krisciunas Fig. 4.



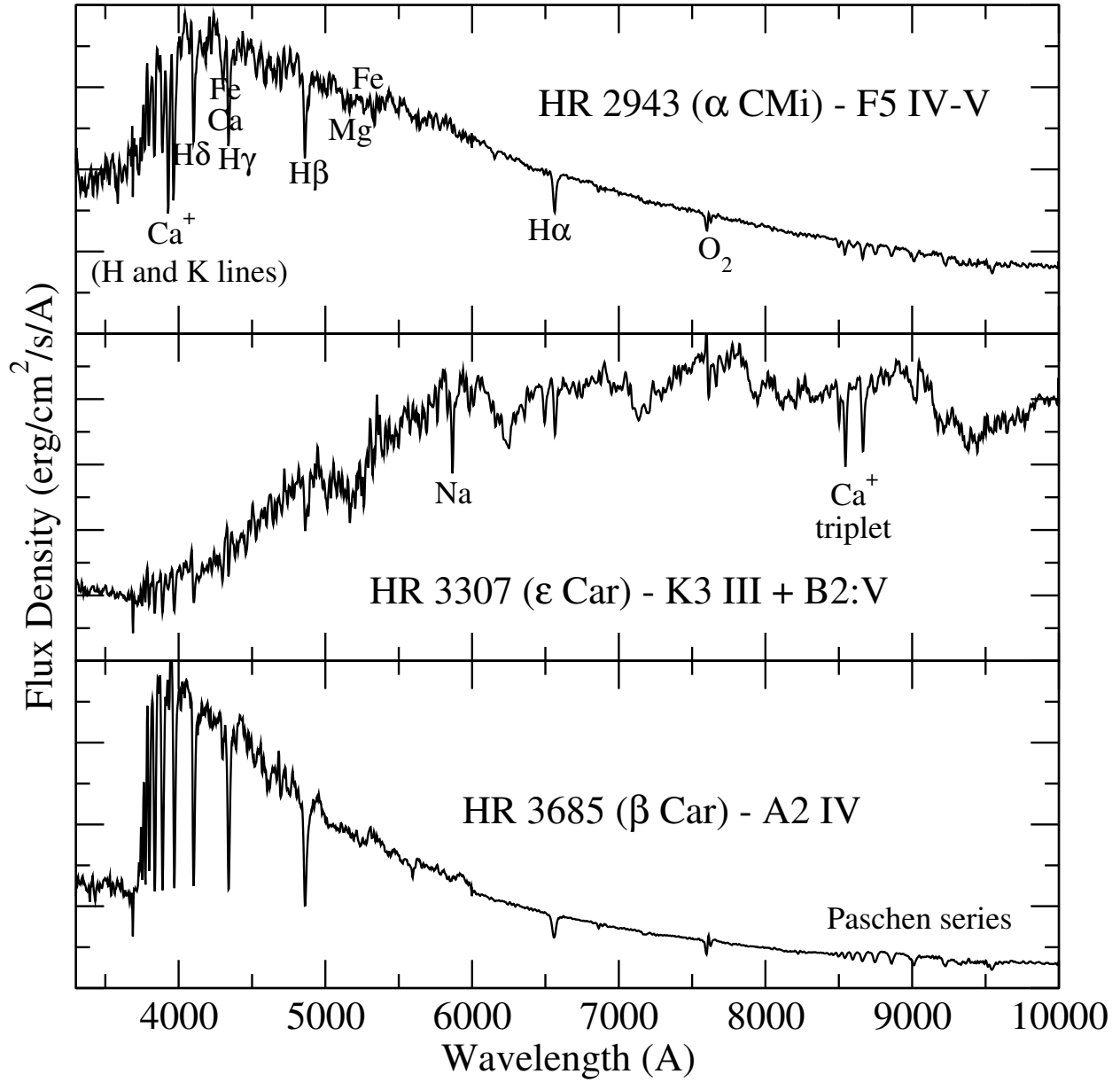
Krisciunas *et al.* Fig. 5



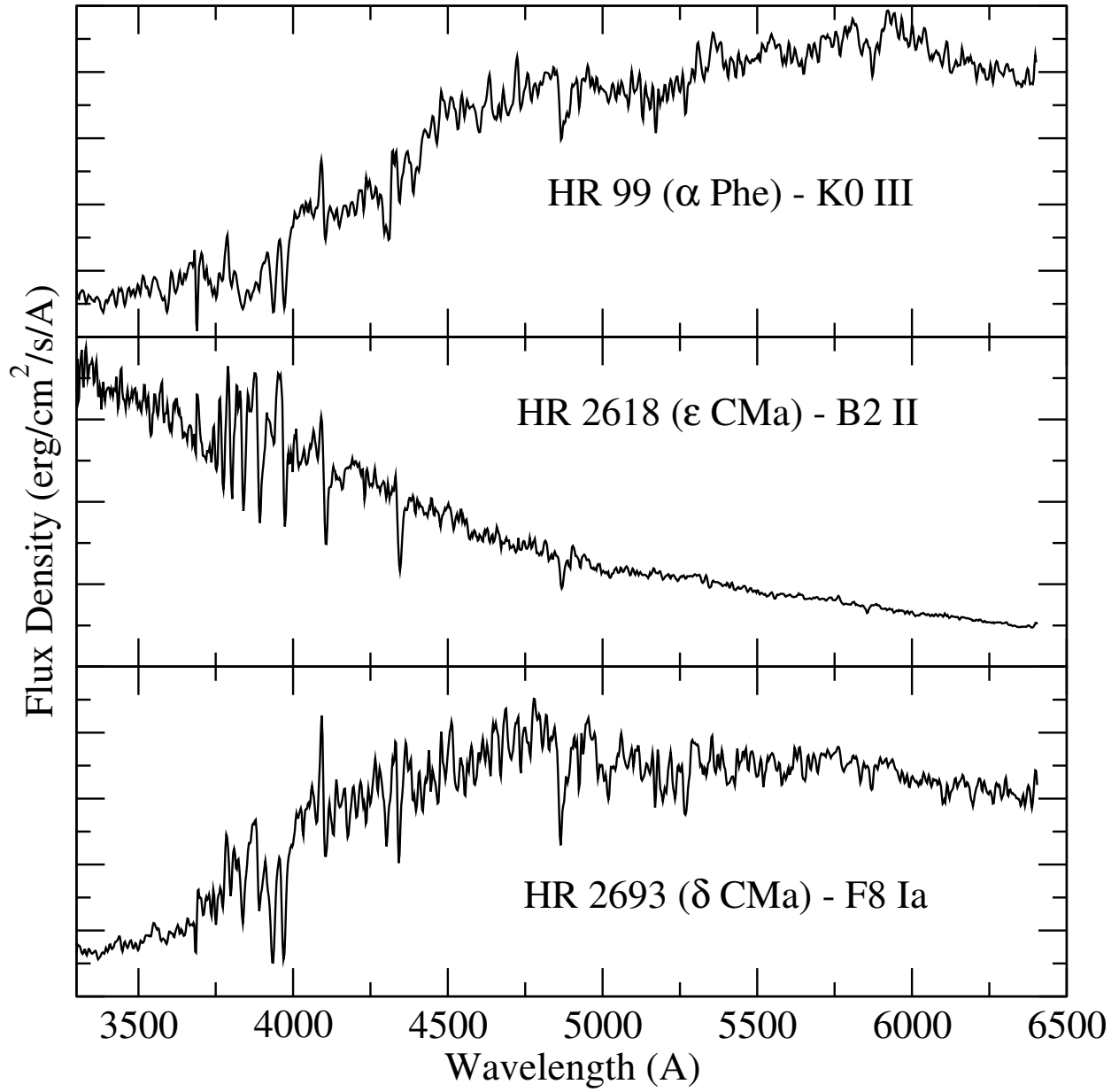
Krisciunas *et al.* Fig. 5 (Continued)



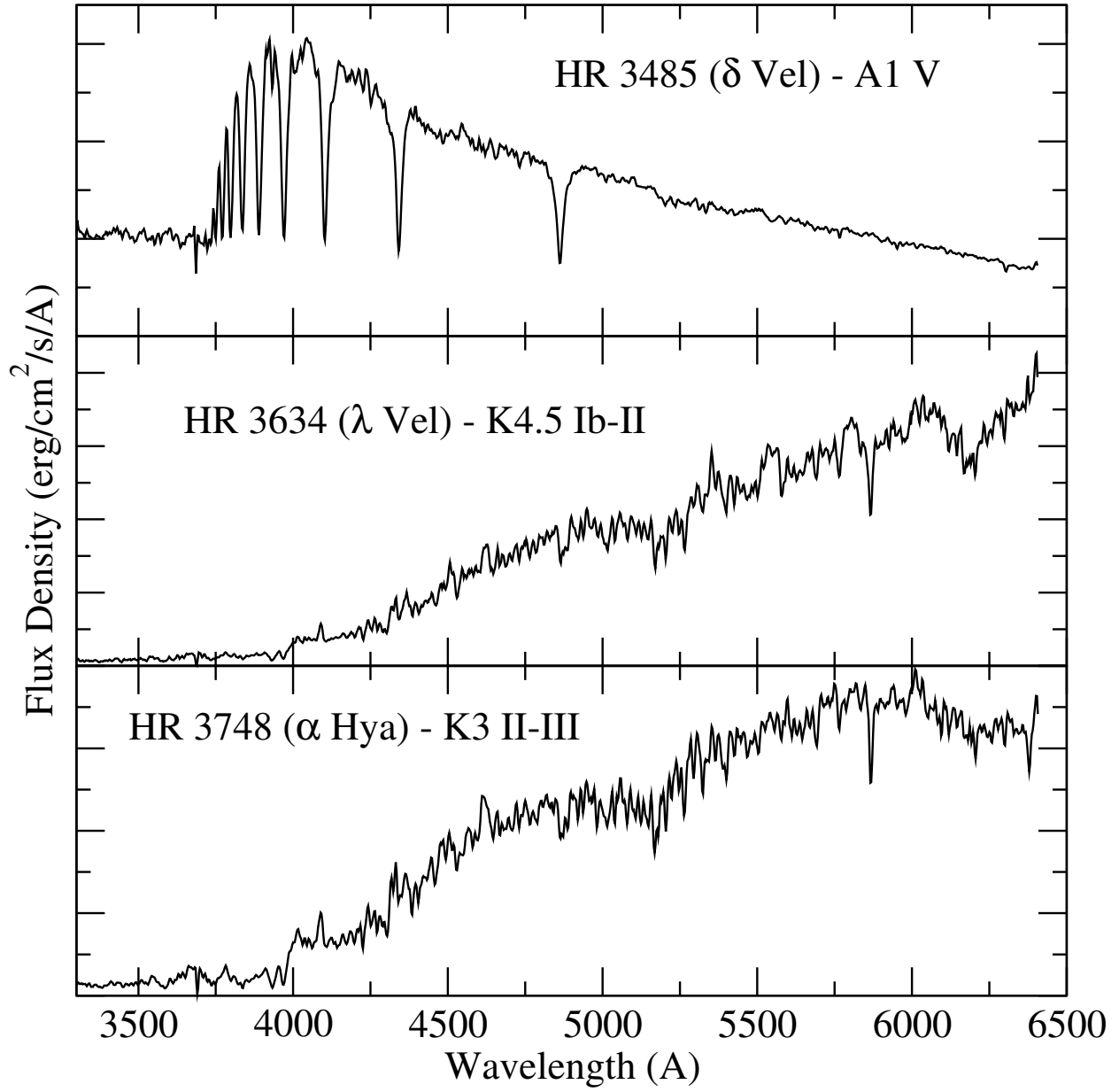
Krisciunas *et al.* Fig. 5 (Continued)



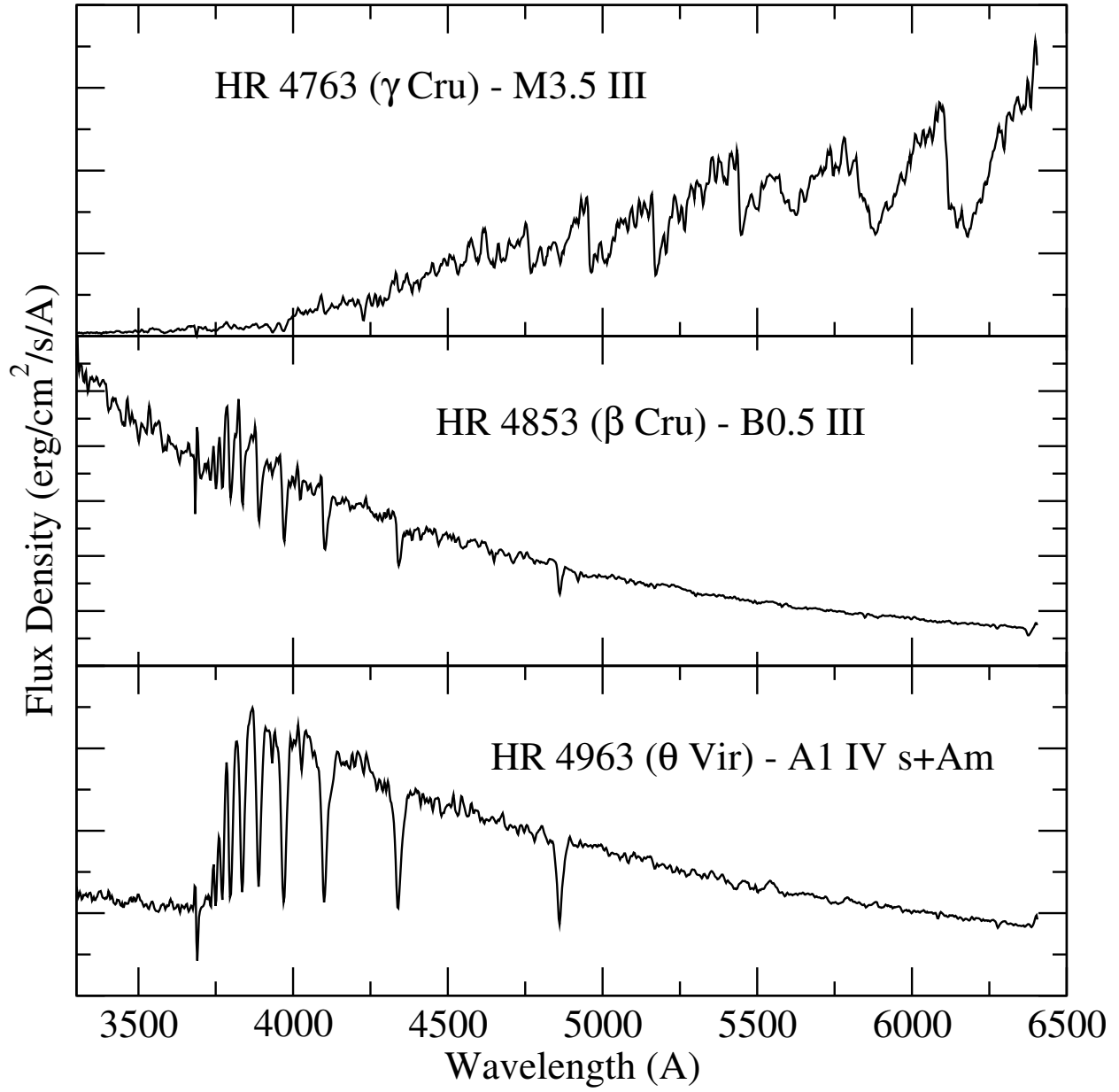
Krisciunas *et al.* Fig. 5 (Continued)



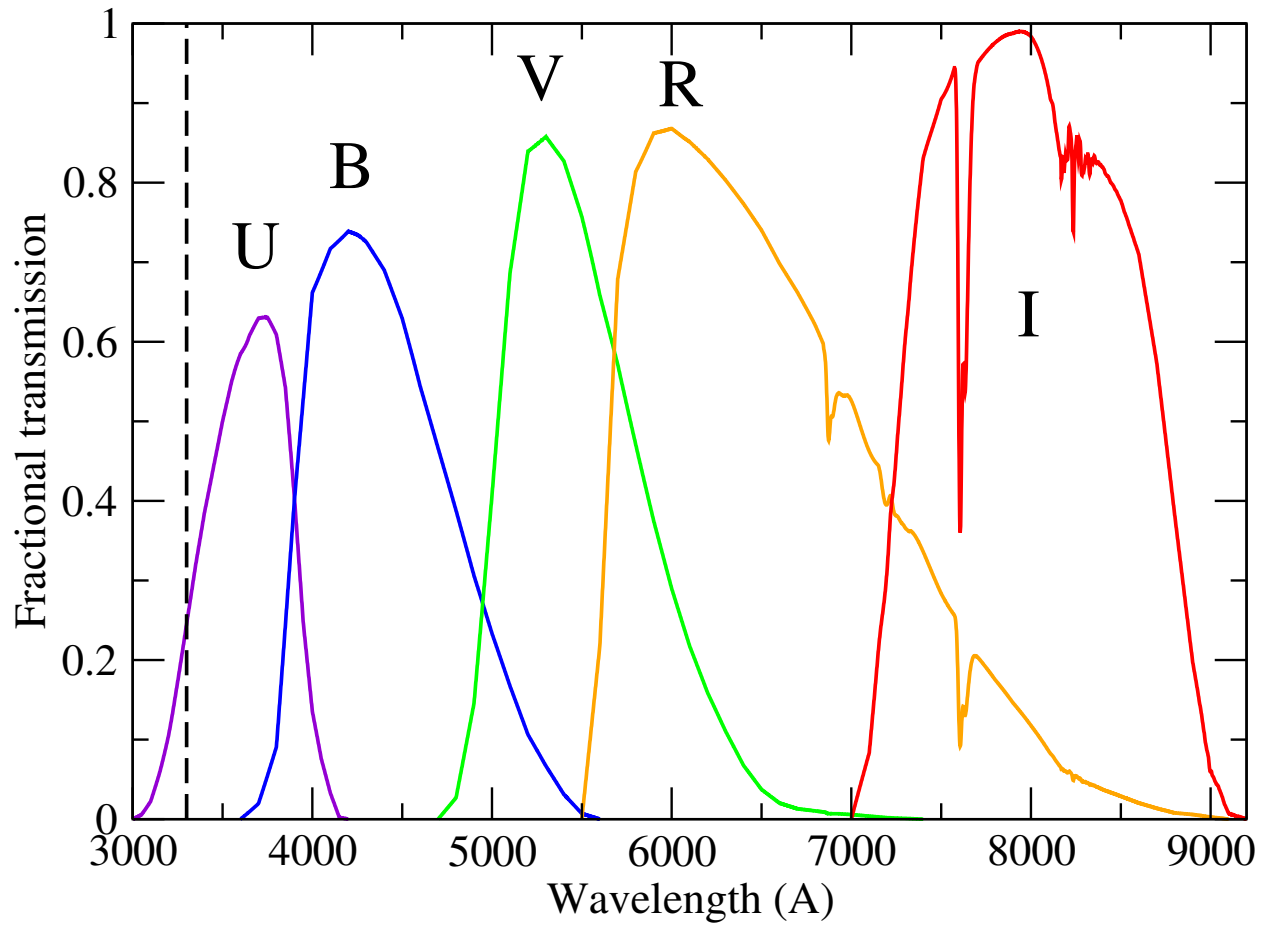
Krisciunas *et al.* Fig. 6



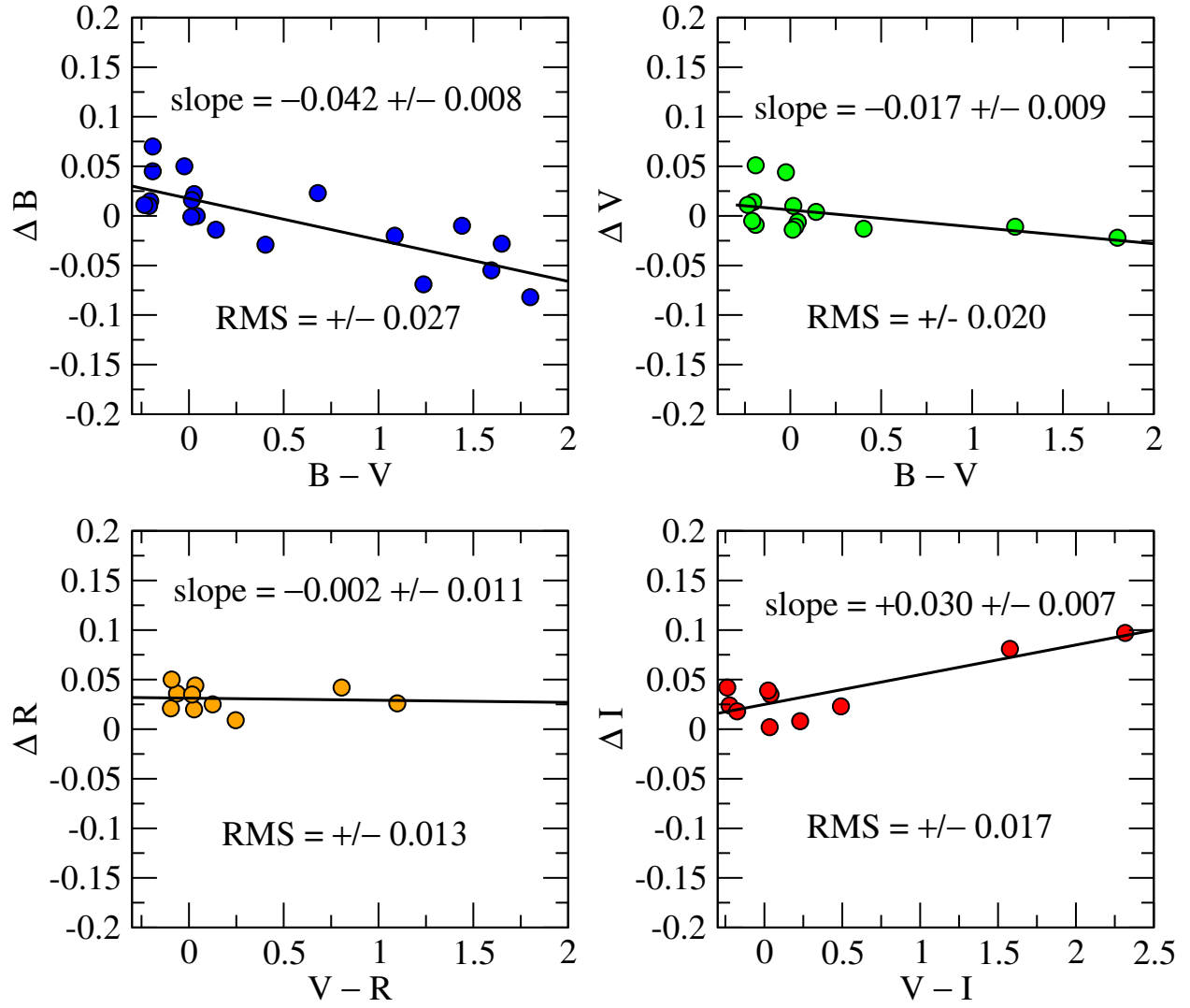
Krisciunas *et al.* Fig. 6 (Continued)



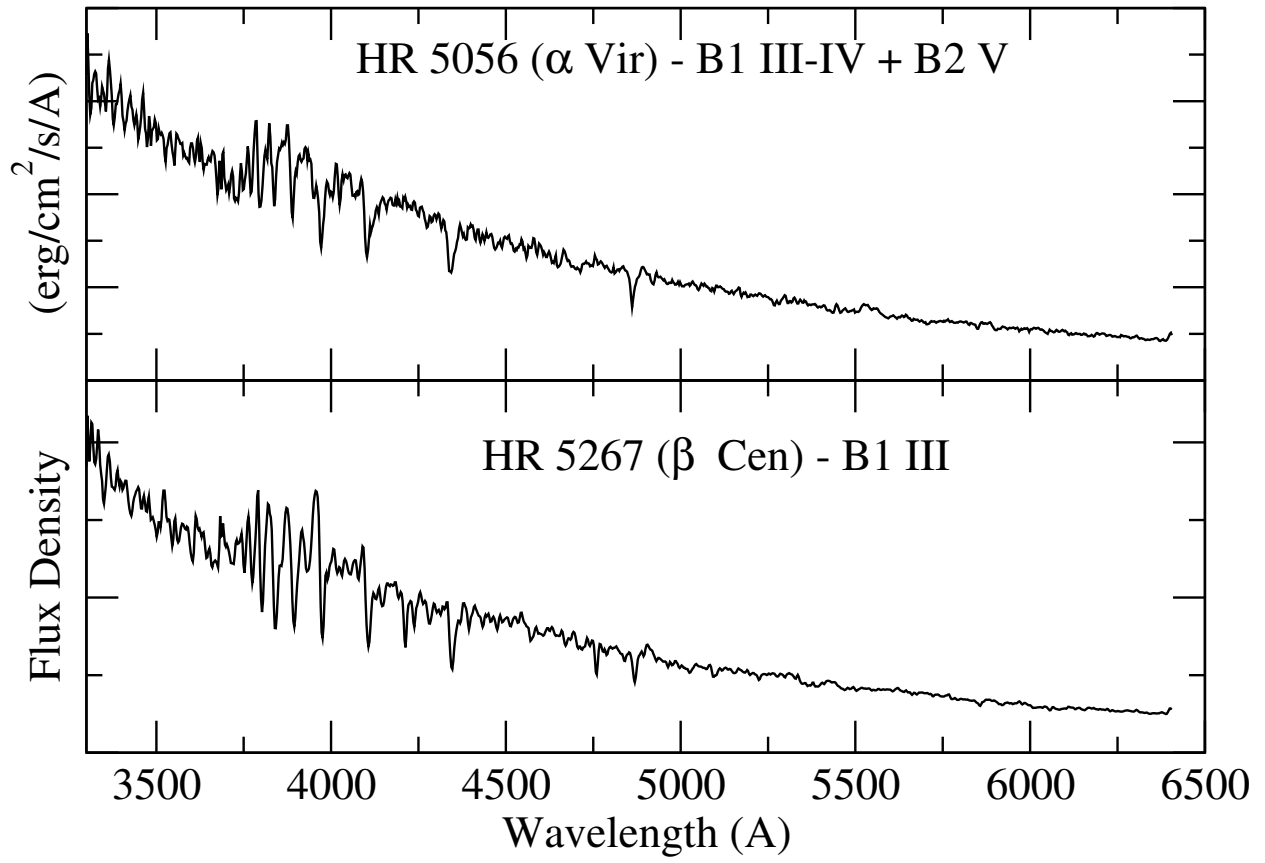
Krisciunas *et al.* Fig. 6 (Continued)



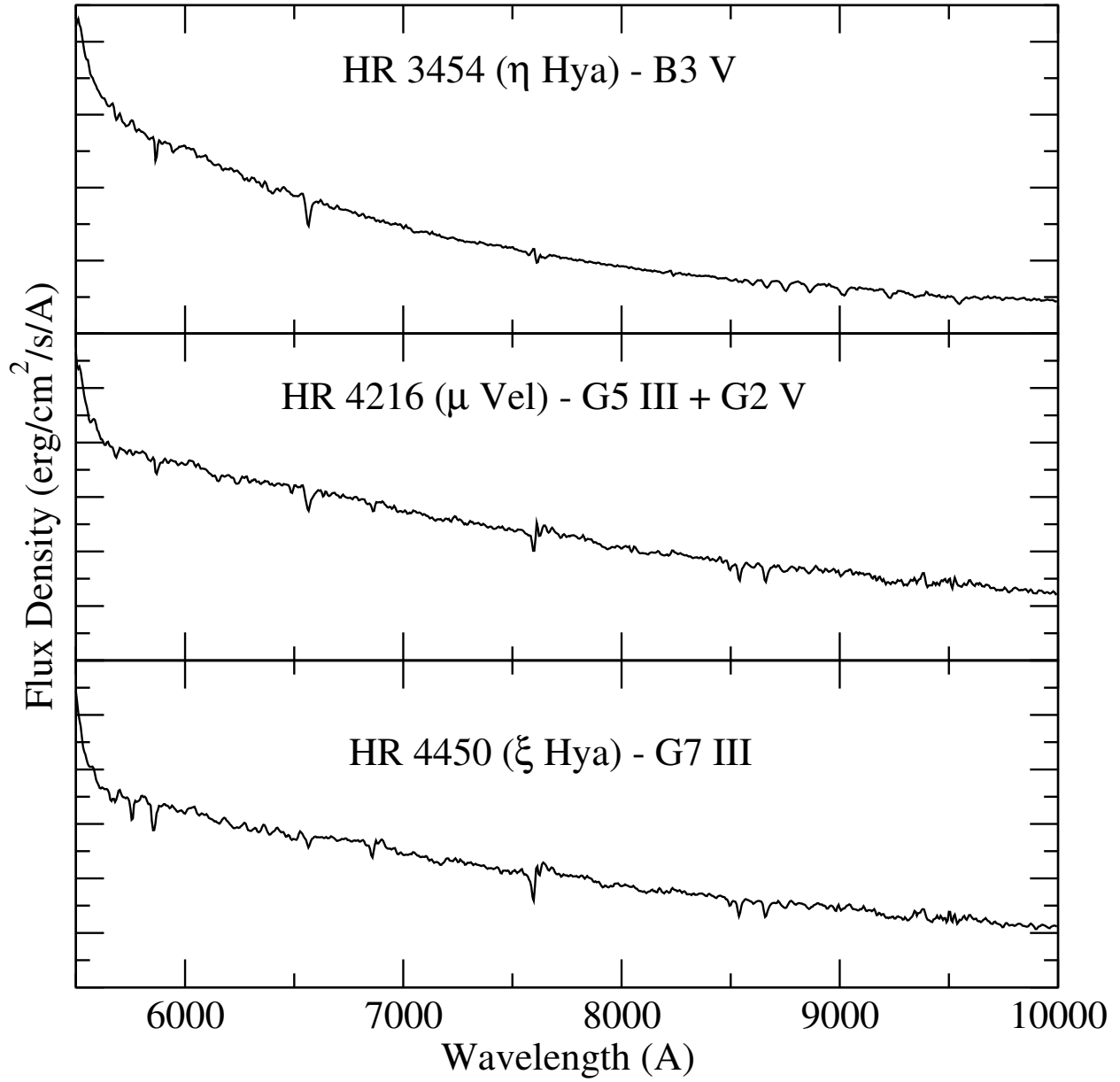
Krisciunas Fig. 7.



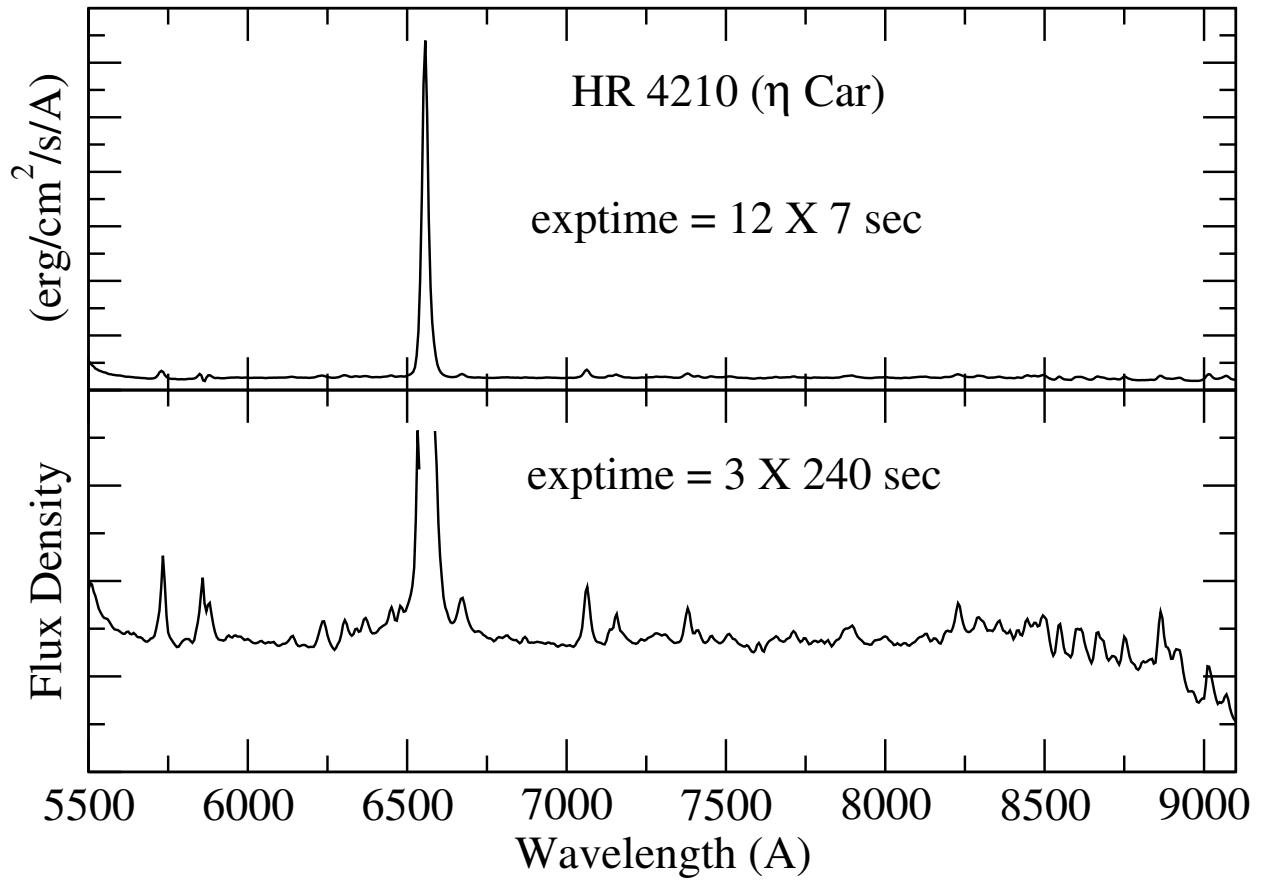
Krisciunas Fig. 8.



Krisciunas Fig. 9.



Krisciunas Fig. 10.



Krisciunas Fig. 11.